International Journal of
Science and Engineering Investigations vol. 6, issue 60, January 2017
ISSN: 2251-8843

Transient Thermal Stress Analyses of Concrete Columns as a Sensible Thermal Energy Storage Medium and a Heater

Sebahattin Ünalan[1], Evrim Özrahat[2], Esen Dağaşan[3]
[1]Department of Mechanical Engineering, Erciyes University, Kayseri, Turkiye
[2]Department of Biosystems Engineering, Bozok University, Yozgat, Turkiye
[3]Department of Material Science Engineering, Erciyes University, Kayseri, Turkiye
([1]s-unalan@erciyes.edu.tr)

Abstract- This paper investigated the thermal stress distribution of a concrete column used as a sensible thermal energy storage medium and a heater. An analytical solution of transient thermal stress distribution in the hollow cylinder concrete columns exposed to heat charging and discharging processes in a period of 24 hours was presented. Transient thermal calculations were carried out for three types of concrete with compressive strength of 18 MPa, 30 MPa and 60 MPa. The results are very attractive in terms of the building heating systems of the future. The investigated concrete columns exposed to extra thermal stress (compressive) values of maximum 7, 10 and 14 MPa for the temperature ranges providing enough heating of the sample flat and thermal comfort.

Keywords- *Transient Thermal Stress, Concrete Column, Heater Column, Sensible Thermal Energy Storage*

I. INTRODUCTION

Investigation of buildings with high thermal energy storage capacity has become one of the hottest topics in the fields of thermal energy engineering and building industry. The thermal energy could be stored as latent heat with phase change materials (PCMs) and sensible heat with materials having high storage capacity. For latent heat energy storage in buildings, the use of PCMs in floors, roofs, walls, and ceiling of a building has been investigated extensively in literature [1-8]. The concrete is an important construction element of the building; moreover researchers are interested in using concrete as a thermal storage medium for a long time. However, as mentioned above, most of the studies were made over latent heat storage in concrete with PCMs. Only a few studies used concrete without PCMs as a sensible heat storage material for building heating and cooling applications. Whereas sensible thermal energy storage in concrete without PCMs would be more attractive than those of concrete with PCMs, because of the potential of being able to use present building materials with well-known physical properties.

A sensible thermal energy storage technology for building applications which uses the building's thermal mass is called as Thermally Activated Building Systems (TABS) [9]. These systems were reviewed extensively in literature. They are defined as heating and cooling systems integrated in the building structure and actively used for heat transfer and heat storage. They mainly exchange heat through radiation and are able to store heat in the building thermal mass. Water pipes or air ducts are embedded in the building surfaces or in the building structure to work as heat exchangers transferring heat to the building rooms and storing thermal energy into the structure. These systems are divided into five categories as radiant floor, radiant ceiling, hollow core slabs, concrete core and pipe-embedded envelopes [9].

In another study, the storage possibility of sensible thermal energy in only concrete columns of multi-storey buildings and the heating performance of the indoors with the stored energy was investigated [10]. Storing the thermal energy in building components such as the wall, floor, ceiling and beams is not considered because of the risk of thermal bridges and design challenges. The hollow concrete column is assumed to have cylindrical geometry. Transient calculations were carried out for an averaged column cross-section of the sample flat and thermal performance and the temperature distributions of the concrete column is discussed. The results show that columns satisfy the heating demand of a sample flat for various air flow velocities and low flow temperatures (< 360 K). In this study, the columns are heated periodically in a day period like conventional heating systems. Therefore, all building columns that carry dynamic and static loads were exposed to extra loads such as thermal stresses and thermal fatigues as a function of the temperature distribution in the column [10]. The aim of the present study is calculating the extra loads (thermal stresses) caused by the transient temperature gradients calculated in the previous study [10]. It is important to know the approximate values of thermal loads for the future experimental studies.

In literature, the transient thermal stress problem in hollow cylinders has been studied analytically and numerically [11-15]. A set of analytical solutions with several new features has been developed for the temperature field and the associated elastic thermal stress distributions for a hollow circular cylinder subjected to sinusoidal transient thermal loading at the inner surface. The approach uses a finite Hankel transform and some properties of Bessel functions [11]. Thermo elasticity problem in a thick-walled cylinder is solved analytically using

the finite Hankel transform. Time-dependent thermal boundary conditions are assumed to act on the inner surface of the cylinder. For the mechanical boundary conditions two different cases are assumed: Traction–displacement problem (traction is prescribed on the inner surface and the fixed displacement boundary condition on the outer one) and Traction–Traction problem (tractions are prescribed on both the inner and outer surfaces of the hollow cylinder). The quasi-static solution of the thermo elasticity problem is derived analytically, i.e., the transient thermal response of the cylinder is derived and then, quasi-static structural problem is solved and closed form relations are extracted for the thermal stresses in the two problems [12]. A study, proposes an extension of the known analytical solution for the temperature and stresses in the event of a linear shock in a pipe containing a fluid was presented. The intention is to propose a simple solution for any variation of the temperature in the fluid and to cover the influence of cladding on the inner surface. The approach consists of breaking down the fluid temperature variation into a succession of linear shocks [13]. There have also been numerical methods to describe the transient behaviors of hollow cylinders under different boundary conditions. A complete analysis of thermal stresses within a thick-walled cylinder under dynamic internal temperature gradient is studied and a complete evaluation of temperature and stress distributions, in a non-steady state, is obtained using a numerical model [14]. The transient thermal response of a thick orthotropic hollow cylinder with finite length is studied by a high order shell theory. The radial and axial displacements are assumed to have quadratic and cubic variations through the thickness, respectively. The equations of motion are derived from the integration of the equilibrium equations of stresses, which are solved by precise integration method [15].

In the previous work [10], time dependent temperature distribution for convective boundary conditions in both inner and outer surface of the hollow concrete body was derived. Thereby the same temperature distribution will be also used in this study to obtain a complete solution of thermal stress analyses of hollow cylinder concrete columns.

II. PROBLEM DESCRIPTION

Instead of traditional heating systems, a new heating system based on column surfaces is considered. Also a new mission was installed on the columns carrying the building's static and dynamic loads in the proposed system. Schematics of the proposed system and probable heat transfer mechanisms can be seen in Figure 1 [10]. The thermal energy from an energy center will be carried by means of dry air flowing through the internal surface of hollow concrete columns. In the proposed system, while the thermal energy charging process performs for a certain period of the day, the discharging process of the stored thermal energy will perform continuously by natural convection and radiation from the column external surfaces to indoor spaces. The charging and discharging operations or the heating-cooling cycles repeated periodically during all winter months. This new mission needs responds for two important questions from new approach.

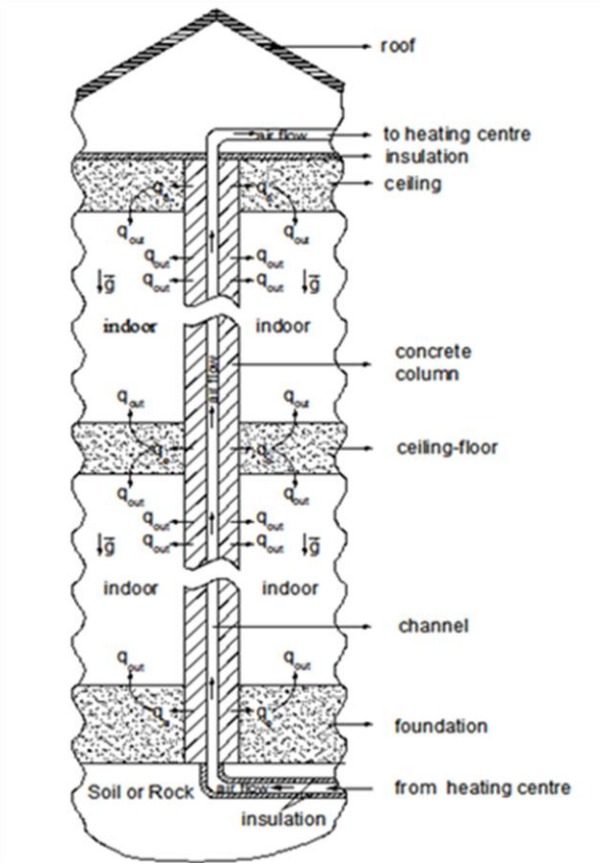

Figure 1. Longitudinal column cross section in building [10].

The first question such as "Is it possible to heat a building by means of the only concrete columns?" was responded positively [10]. The second question "How will the heating-cooling cycles affect the mechanical performance of concrete columns and the life of the building? are needed to be answered, respectively. The first step to answer the second question is to calculate the thermal stress distribution. In this study, the thermal stress as a function of temperature changes during charging and discharging processes of sensible thermal energy on the concrete columns will be investigated. In the investigation, thermal and mechanical properties of columns made of concrete are very important in this stage. The concrete is basically a mixture consist of water, aggregate and cement. The microstructures and grain sizes of the used aggregate and cement paste with different water percentages have a great effect on the strength of the concrete. Thereby, the concrete production and classification in the world cannot be formulated as a function of material composition due to different sizes and microstructures in different regions of the world. Consequently, concrete classification based on the strength of the resulting products assumed. Nowadays, the mechanical and thermo-physical properties of the concrete are determined experimentally after the production. Therefore, there is not an available consensus on thermodynamic and mechanical properties of the concrete over the world. For this study, it is

useful to divide concrete into three general categories based on compressive strength [16]:

1. Low-strength concrete [LSC]: less than 20 MPa (3000 psi)

2. Moderate-strength concrete [MSC]: 20 to 40 MPa (3000 to 6000 psi)

3. High-strength concrete [HSC]: more than 40 MPa (6000 psi).

Typical proportions of materials for producing low-strength, moderate strength and high-strength concrete mixtures with normal-weight aggregate are shown in Table 1 [16].The calculations are realized for three types of concrete of different strength classes given in Table 1. For more reliable results, thermo-physical properties of concrete types are calculated by composite material approach according to the mix proportions given in Table 1. As the concrete is composed of cement paste (cement + water) and aggregate (fine + coarse); it can be assumed as a composite material. Consider a two-phase consisting of a cement paste (1) and aggregate (2), the locally effective bulk modulus K and shear modulus μ are given by the Mori–Tanaka estimation [17,18] as:

$$\frac{K-K_1}{K_2-K_1}=\frac{V_2}{1+(1-V_2)\frac{K_2-K_1}{K_1+\frac{4}{3}\mu_1}} \quad (1)$$

$$\frac{\mu-\mu_1}{\mu_2-\mu_1}=\frac{V_2}{1+(1-V_2)\frac{\mu_2-\mu_1}{\mu_1+f_1}} \quad (2)$$

$$f_1=\frac{\mu_1(9K_1+8\mu_1)}{6(K_1+2\mu_1)} \quad (3)$$

Where *V* denotes the volume fractions and is related by:

$$V_1+V_2=1 \quad (4)$$

The coefficient of thermal expansion α is determined in terms of the correspondence relation [22-25]:

$$\frac{\alpha-\alpha_1}{\alpha_2-\alpha_1}=\frac{\frac{1}{K}-\frac{1}{K_1}}{\frac{1}{K_2}-\frac{1}{K_1}} \quad (5)$$

The locally effective heat conductivity coefficient k is given by [26]:

$$\frac{k-k_1}{k_2-k_1}=\frac{V_2}{1+(1-V_2)\frac{k_2-k_1}{3k_1}} \quad (6)$$

In the CEB-FIP Model Code (1990), the modulus of elasticity of normal-weight concrete can be estimated from [19]:

$$E_c=2.15*10^4(f_{cm}/10)^{1/3} \quad (7)$$

Where Ec is the 28-day modulus of elasticity of concrete (MPa) and f_{cm} is the average 28-day compressive strength. The elastic modulus-strength relationship was developed for quarzitic aggregate concrete. For other types of aggregates, the modulus of elasticity can be obtained by multiplying E_c with factors a_c which is defined as 1.2 for limestone.

Poisons ratio of the concrete lies generally in the range of 0.15 to 0.22 [24]. There appears to be no consistent relationship between Poisson's ratio and concrete characteristics such as water-cement ratio, curing age, and aggregate gradation. However, Poisson's ratio is generally lower in high-strength concrete [16].

TABLE I. TYPICAL PROPORTIONS OF MATERIALS IN CONCRETE MIXTURES OF DIFFERENT STRENGTH [16].

Concrete Types	*Low-strength (kg/m³)*	*Moderate-strength (kg/m³)*	*High-strength (kg/m³)*
Cement	255	356	510
Water	178	178	178
Fine aggregate	801	848	890
Course aggregate	1.169	1.032	872
Cement paste proportion			
percent by mass	18,0	22,1	28,1
percent by volume	0.260	0.293	0.343
Water/cement by mass	0,7	0,5	0,3
Strength (MPa)	18	30	60

Therefore the poisons ratio is chosen as 0.22, 0.19 and 0.15 for low-strength, moderate-strength and high-strength concrete respectively. When fine and course aggregate is from the same rock type, the specific gravity of aggregate can be easily calculated according to the Table 1 as 2.66, 2.66 and 2.68 for low-strength, moderate-strength and high-strength concrete respectively. Therefore the aggregate type is found as limestone from the literature [24]. In three types of concrete, aggregate is the same as limestone but the cement paste differs in water cement ratio (w/c) as 0.7, 0.5 and 0.3 for low-strength, moderate-strength and high-strength concrete respectively. Thermal properties of the concrete can be estimated from the properties of aggregate and cement paste of different w/c ratios. Thermal properties of aggregates and cement pastes collected from literature are given in Table 2. Using the equations (1-7) physical and mechanical properties of three types of concrete is calculated and given in Table 3.

III. ANALYTICAL SOLUTION

In this study, the main aim is to calculate the transient thermal stress distribution as a function of temperature ranges required for enough heating of a flat on an average column analytically. As the temperature distributions for various energy charging and energy discharging conditions are obtained in the previous study [10], thermal stress distribution corresponding to those temperatures will be obtained in this work. For the more simplified solution, plaster, iron, pipe, special pipe system, paint layer, walls and beams connected with the column are ignored in analytical solution. In addition, the rectangular column section was assumed to have a cylindrical geometry. For simplicity, the transient calculations in the cylindrical geometry in Figure 2 are carried out in 1-dimensional cylindrical coordinates. Transient calculations were carried out for consecutive different intervals. At the first time period of Δt_1 (corresponding to the daytime), both energy charging and discharging process occurs simultaneously. At the period of the Δt_1, the energy charging process cancels. A part of the stored thermal energy transfers to indoors during the

operation period of the followed Δt_2 (corresponding to night hours). Then, the energy charge process again starts at the period of the Δt_3 (corresponding to the daytime of the following day). The explained cycles repeated during the winter.

TABLE II. THERMAL PROPERTIES OF AGGREGATES AND CEMENT PASTES

	aggregate (limestone)	*cement paste (w/c=0.7)*	*cement paste (w/c=0.5)*	*cement paste (w/c=0.3)*
Thermal conductivity (W/mK)	2,7[25]	0,7[26]	1,07[26]	1,1[26]
Thermal expansion coefficient (per °C)	0,000005 [16]	0,000018 [16]	0,000018 [16]	0,000018 [16]

TABLE III. PHYSICAL AND MECHANICAL PROPERTIES OF THREE TYPES OF CONCRETE

	Low-strength concrete	*Moderate-strength concrete*	*High-strength concrete*
Dry density (kg/m3)	2225	2236	2272
E (MPa)	23538	27907	35161
Poisson ratio	0.22	0.19	0.15
Thermal conductivity (W/mK)	2.55	2.39	2.33
Thermal expansion coefficient (per °C)	7.47E-06	7.99E-06	8.80E-06
Specific heat (J/kg K)	969	924	912

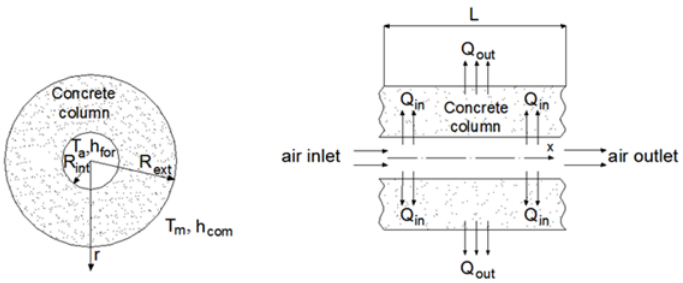

Figure 2. Cylindrical column cross section for analytical solution [10].

For the calculations, temperatures of the dry air flowing in the hollow column and indoors are assumed as constant Ta and Tm, respectively. The temperature distribution in the concrete column can be governed by following differential equation, boundary and initial conditions:

$$\frac{1}{r}\frac{\partial T}{\partial r}+\frac{\partial^2 T}{\partial r^2}=\frac{1}{\alpha}\frac{\partial T}{\partial t} \quad (8)$$

For the first energy charging (indicated by I upper script) during time period of $\Delta t1$, boundary and initial conditions are as follows:

$$-k\left(\frac{\partial T^I}{\partial r}\right)_{r=R_{ext}}=h_{com}[T^I-T_m]_{r=R_{ext}} \quad (9)$$

$$-k\left(\frac{\partial T^I}{\partial r}\right)_{r=R_{int}}=h_{for}[T_a-T^I]_{r=R_{int}} \quad (10)$$

$$T^I(r,0)=T_m \quad (11)$$

For the energy discharging (indicated by II upper script) during time period of $\Delta t2$, boundary and initial conditions are as follows:

$$-k\left(\frac{\partial T^{II}}{\partial r}\right)_{r=R_{ext}}=h_{com}[T^{II}-T_m]_{r=R_{ext}} \quad (12)$$

$$-k\left(\frac{\partial T^{II}}{\partial r}\right)_{r=R_{int}}=0 \quad (13)$$

$$T^{II}(r,0)=T^I(r,\Delta t_1) \quad (14)$$

For the second energy charging (indicated by III upper script) during time period of $\Delta t1$, boundary and initial conditions are as follows:

$$-k\left(\frac{\partial T^{III}}{\partial r}\right)_{r=R_{ext}}=h_{com}[T^{III}-T_m]_{r=R_{ext}} \quad (15)$$

$$-k\left(\frac{\partial T^{III}}{\partial r}\right)_{r=R_{int}}=h_{for}[T_a-T^{III}]_{r=R_{int}} \quad (16)$$

$$T^{III}(r,0)=T^{II}(r,\Delta t_2) \quad (17)$$

In following equations, while the indices indicated by I, III, V, VII … uppers script exhibited energy charging and discharging stages, also indices indicated by II, IV, VI … uppers script exhibited energy discharging stages. Solutions of the partial differential in Eq.1 with given boundary and initial conditions by means of separation of variables method are as follows:

$$T^I(r,t)=\sum_{n=1}^{\infty}C_n^I[J_0(\lambda_n r)+H_n Y_0(\lambda_n r)]e^{-\alpha\lambda_n^2 t}+F_1 lnr+F_2+T_m \quad (18)$$

$$T^{II}(r,t)=\sum_{n=1}^{\infty}C_n^{II}\left[J_0(\beta_n r)-\frac{J_1(\beta_n R_{int})}{Y_1(\beta_n R_{int})}Y_0(\beta_n r)\right]e^{-\alpha\beta_n^2 t}+T_m \quad (19)$$

$$T^{III}(r,t)=\sum_{n=1}^{\infty}C_n^{III}[J_0(\lambda_n r)+H_n Y_0(\lambda_n r)]e^{-\alpha\lambda_n^2 t}+F_1 lnr+F_2+T_m \quad (20)$$

$$T^{IV}(r,t)=\sum_{n=1}^{\infty}C_n^{IV}\left[J_0(\beta_n r)-\frac{J_1(\beta_n R_{int})}{Y_1(\beta_n R_{int})}Y_0(\beta_n r)\right]e^{-\alpha\beta_n^2 t}+T_m \quad (21)$$

$$T^V(r,t)=\sum_{n=1}^{\infty}C_n^V[J_0(\lambda_n r)+H_n Y_0(\lambda_n r)]e^{-\alpha\lambda_n^2 t}+F_1 lnr+F_2+T_m \quad (22)$$

Where Hn, F_1, F_2, C_n^I, C_n^{II}, C_n^{III}, C_n^{IV} and C_n^V can be explained by following equations:

$$F_1=\frac{T_m-T_a}{\frac{k}{h_{com}R_{ext}}+\frac{k}{h_{for}R_{int}}+ln\left(\frac{R_{ext}}{R_{int}}\right)} \quad (23)$$

$$F_2=-F_1\left[ln(R_{ext})+\frac{k}{h_{com}R_{ext}}\right] \quad (24)$$

$$H_n=\frac{h_{com}J_0(\lambda_n R_{ext})-k\lambda_n J_1(\lambda_n R_{ext})}{k\lambda_n Y_1(\lambda_n R_{ext})-h_{com}Y_0(\lambda_n R_{ext})} \quad (25)$$

$$C_n^I = \frac{-\int_{R_{int}}^{R_{ext}} r(F_1 lnr + F_2)[J_0(\lambda_n r) + H_n Y_0(\lambda_n r)]dr}{\int_{R_{int}}^{R_{ext}} r[J_0(\lambda_n r) + H_n Y_0(\lambda_n r)]^2 dr} \quad (26)$$

$$C_n^{II} = \frac{\int_{R_{int}}^{R_{ext}} r(T^I(R,\Delta t_1) - T_m)\left[Y_0(\beta_n r) - \frac{Y_1(\beta_n R_{int})}{J_1(\beta_n R_{int})} J_0(\beta_n r)\right]dr}{\int_{R_{int}}^{R_{ext}} r\left[Y_0(\beta_n r) - \frac{Y_1(\beta_n R_{int})}{J_1(\beta_n R_{int})} J_0(\beta_n r)\right]^2 dr} \quad (27)$$

$$C_n^{III} = \frac{-\int_{R_{int}}^{R_{ext}} r(T^{II}(R,\Delta t_2) - T_m - (F_1 lnr + F_2))[J_0(\lambda_n r) + H_n Y_0(\lambda_n r)]dr}{\int_{R_{int}}^{R_{ext}} r[J_0(\lambda_n r) + H_n Y_0(\lambda_n r)]^2 dr} \quad (28)$$

$$C_n^{IV} = \frac{\int_{R_{int}}^{R_{ext}} r(T^{III}(R,\Delta t_3) - T_m)\left[Y_0(\beta_n r) - \frac{Y_1(\beta_n R_{int})}{J_1(\beta_n R_{int})} J_0(\beta_n r)\right]dr}{\int_{R_{int}}^{R_{ext}} r\left[Y_0(\beta_n r) - \frac{Y_1(\beta_n R_{int})}{J_1(\beta_n R_{int})} J_0(\beta_n r)\right]^2 dr} \quad (29)$$

$$C_n^V = \frac{-\int_{R_{int}}^{R_{ext}} r(T^{IV}(R,\Delta t_4) - T_m - (F_1 lnr + F_2))[J_0(\lambda_n r) + H_n Y_0(\lambda_n r)]dr}{\int_{R_{int}}^{R_{ext}} r[J_0(\lambda_n r) + H_n Y_0(\lambda_n r)]^2 dr} \quad (30)$$

λ_n and β_n eigenvalues (n=1,2,3,4,…) are positive roots calculated by the following equations:

$$\frac{[k\lambda_n Y_1(\lambda_n R_{int}) + h_{for} Y_0(\lambda_n R_{int})][k\lambda_n J_1(\lambda_n R_{ext}) - h_{com} J_0(\lambda_n R_{ext})]}{[h_{for} J_0(\lambda_n R_{int}) + k\lambda_n J_1(\lambda_n R_{int})][k\lambda_n Y_1(\lambda_n R_{ext}) - h_{com} Y_0(\lambda_n R_{ext})]} = 1 \quad (31)$$

$$\frac{Y_1(\beta_n R_{int})[k\beta_n J_1(\beta_n R_{ext}) - h_{com} J_0(\beta_n R_{ext})]}{J_1(\beta_n R_{int})[k\beta_n Y_1(\beta_n R_{ext}) - h_{com} Y_0(\beta_n R_{ext})]} = 1 \quad (32)$$

The temperature variation and total heat transfer rates in the internal (Qin) and external surfaces (Qout) of the hollow column can be explained as a function of the operation time.

$$Q_{out}(t) = 2\pi R_{ext} n_c L h_{com}[T(R_{ext}, t) - T_m] \quad (33)$$

$$Q_{in}(t) = 2\pi R_{int} n_c L h_{for}[T_a - T(R_{int}, t)] \quad (34)$$

$$T_{int}(t) = T(R_{int}, t) \quad (35)$$

$$T_{out}(t) = T(R_{ext}, t) \quad (36)$$

For the C_n values calculations from Eqs.26-30, the integrals in the equations can be solved by two methods. First method can be numerical integration. However, the numerical integration may cause numerical errors. Thereby, the integrals in (26-30) have to be solved analytically as a second method. The new forms of (26-30) with solved integrals are as follows:

$$f_1(x,n) = J_0(x) + H_n Y_0(x) \quad (37)$$

$$f_2(x,n) = J_1(x) + H_n Y_1(x) \quad (38)$$

$$f_3(x,n) = J_0(x) - \frac{J_1(\beta_n R_{int})}{Y_1(\beta_n R_{int})} Y_0(x) \quad (39)$$

$$f_4(x,n) = J_1(x) - \frac{J_1(\beta_n R_{int})}{Y_1(\beta_n R_{int})} Y_1(x) \quad (40)$$

$$fb(x,n) = \frac{x^2}{2(\lambda_n)^2}[[f_1(x,n)]^2 + [f_2(x,n)]^2] \quad (41)$$

$$ft(x,n) = \frac{(F_1 \ln(\lambda_n) - F_2)x}{(\lambda_n)^2} f_2(x,n) - \frac{F_1}{(\lambda_n)^2}(xlnx f_2(x,n) + f_1(x,n)) \quad (42)$$

$$fb1(x,n) = \frac{x^2}{2(\beta_n)^2}[[f_3(x,n)]^2 + [f_4(x,n)]^2] \quad (43)$$

$$ft1(x,n) = \frac{-(F_1 \ln(\beta_n) - F_2)x}{(\beta_n)^2} f_4(x,n) + \frac{F_1}{(\beta_n)^2}(xlnx f_4(x,n) + f_3(x,n)) \quad (44)$$

$$C_n^0 = \frac{ft1(\beta_n R_{ext},n) - ft1(\beta_n R_{int},n)}{fb1(\beta_n R_{ext},n) - fb1(\beta_n R_{int},n)} \quad (45)$$

$$ft2(r,n) = \sum_{i=1}^{\infty} \frac{C_i^I r e^{-\alpha\lambda_i^2 \Delta t_1}}{(\lambda_i)^2 - (\beta_n)^2}\left(\lambda_i f_3(\beta_n r, n) f_2(\lambda_i r, i) - \beta_n f_4(\beta_n r, n) f_1(\lambda_i r, i)\right) \quad (46)$$

$$ft3(r,n) = \sum_{i=1}^{\infty} \frac{C_i^{II} r e^{-\alpha\beta_i^2 \Delta t_2}}{(\lambda_n)^2 - (\beta_i)^2}\left(\lambda_n f_3(\beta_i r, i) f_2(\lambda_n r, n) - \beta_i f_4(\beta_i r, i) f_1(\lambda_n r, n)\right) \quad (47)$$

$$ft4(r,n) = \sum_{i=1}^{\infty} \frac{C_i^{III} r e^{-\alpha\lambda_i^2 \Delta t_3}}{(\lambda_i)^2 - (\beta_n)^2}\left(\lambda_i f_3(\beta_n r, n) f_2(\lambda_i r, i) - \beta_n f_4(\beta_n r, n) f_1(\lambda_i r, i)\right) \quad (48)$$

$$ft5(r,n) = \sum_{i=1}^{\infty} \frac{C_i^{IV} r e^{-\alpha\beta_i^2 \Delta t_4}}{(\lambda_n)^2 - (\beta_i)^2}\left(\lambda_n f_3(\beta_i r, i) f_2(\lambda_n r, n) - \beta_i f_4(\beta_i r, i) f_1(\lambda_n r, n)\right) \quad (49)$$

$$C_n^I = \frac{ft(\lambda_n R_{ext},n) - ft(\lambda_n R_{int},n)}{fb(\lambda_n R_{ext},n) - fb(\lambda_n R_{int},n)} \quad (50)$$

$$C_n^{II} = C_n^0 + \frac{ft2(R_{ext},n) - ft2(R_{int},n)}{fb1(\beta_n R_{ext},n) - fb1(\beta_n R_{int},n)} \quad (51)$$

$$C_n^{III} = C_n^I + \frac{ft3(R_{ext},n) - ft3(R_{int},n)}{fb(\lambda_n R_{ext},n) - fb(\lambda_n R_{int},n)} \quad (52)$$

$$C_n^{IV} = C_n^0 + \frac{ft4(R_{ext},n) - ft4(R_{int},n)}{fb1(\beta_n R_{ext},n) - fb1(\beta_n R_{int},n)} \quad (53)$$

$$C_n^V = C_n^I + \frac{ft5(R_{ext},n) - ft5(R_{int},n)}{fb(\lambda_n R_{ext},n) - fb(\lambda_n R_{int},n)} \quad (54)$$

In the thermal stress calculations, it is assumed that the concrete hollow cylinder is made of a homogeneous isotropic material. The hollow cylinder is considered to be sufficiently long in its axial direction to apply the hypothesis of plain strain. In addition, it is assumed that the thermos-mechanical properties do not change during energy charge and discharge stages and that the strain rates due to the thermal loading are small, so both the inertia and thermos-mechanical coupling terms in the thermos-elasticity governing equations can be neglected. On this basis an analytical solution for the stress components will be specified for a hollow cylinder with appropriate boundary conditions. Applying the boundary conditions for traction free surfaces (σ_r=0 at r=R_{int} and r=R_{ext}) for radial direction and εz=ε0 condition (free end) for z direction [11, 14, 27], then stress components (σ_r: radial stress, σ_θ: hoop stress, σ_z: axial stress) are obtained as follows:

$$\sigma_r(r,t) = \frac{\alpha E}{1-\vartheta}\frac{1}{r^2}\left[-\int_{R_{int}}^{r} \theta(r,t) r dr + \frac{r^2 - R_{int}^2}{R_{ext}^2 - R_{int}^2}\int_{R_{int}}^{R_{ext}} \theta(r,t) r dr\right] \quad (55)$$

$$\sigma_\theta(r,t) = \frac{\alpha E}{1-\vartheta}\frac{1}{r^2}\left[+\frac{r^2 + R_{int}^2}{R_{ext}^2 - R_{int}^2}\int_{R_{int}}^{R_{ext}} \theta(r,t) r dr - r^2\theta(r,t)\right] \quad (56)$$

$$\sigma_z(r,t) = \frac{\alpha E}{1-\vartheta}\left[\frac{2}{R_{ext}^2 - R_{int}^2}\int_{R_{int}}^{R_{ext}} \theta(r,t) r dr - \theta(r,t)\right] \quad (57)$$

Where θ (r,t) =T(r,t)-T_m. When the above equations are integrated by substituting the temperature distributions

obtained for different stages, the following stress components are obtained:

$$\sigma_\theta^I(r,t) = \frac{\alpha E}{1-\vartheta}\frac{1}{r^2}\left[\frac{r^2+R_{int}^2}{R_{ext}^2-R_{int}^2}G_1^I(t) + G_2^I(r,t) - r^2(T^I(r,t)-T_m)\right] \quad (58)$$

$$\sigma_\theta^{II}(r,t) = \frac{\alpha E}{1-\vartheta}\frac{1}{r^2}\left[\frac{r^2+R_{int}^2}{R_{ext}^2-R_{int}^2}G_1^{II}(t) + G_2^{II}(r,t) - r^2(T^{II}(r,t)-T_m)\right] \quad (59)$$

$$\sigma_\theta^{III}(r,t) = \frac{\alpha E}{1-\vartheta}\frac{1}{r^2}\left[\frac{r^2+R_{int}^2}{R_{ext}^2-R_{int}^2}G_1^{III}(t) + G_2^{III}(r,t) - r^2(T^{III}(r,t)-T_m)\right] \quad (60)$$

$$\sigma_\theta^{IV}(r,t) = \frac{\alpha E}{1-\vartheta}\frac{1}{r^2}\left[\frac{r^2+R_{int}^2}{R_{ext}^2-R_{int}^2}G_1^{IV}(t) + G_2^{IV}(r,t) - r^2(T^{IV}(r,t)-T_m)\right] \quad (61)$$

$$\sigma_\theta^{V}(r,t) = \frac{\alpha E}{1-\vartheta}\frac{1}{r^2}\left[\frac{r^2+R_{int}^2}{R_{ext}^2-R_{int}^2}G_1^{V}(t) + G_2^{V}(r,t) - r^2(T^{V}(r,t)-T_m)\right] \quad (62)$$

$$\sigma_r^I(r,t) = \frac{\alpha E}{1-\vartheta}\frac{1}{r^2}\left[\frac{r^2-R_{int}^2}{R_{ext}^2-R_{int}^2}G_1^I(r,t) - G_2^I(r,t)\right] \quad (63)$$

$$\sigma_r^{II}(r,t) = \frac{\alpha E}{1-\vartheta}\frac{1}{r^2}\left[\frac{r^2-R_{int}^2}{R_{ext}^2-R_{int}^2}G_1^{II}(t) + G_2^{II}(r,t)\right] \quad (64)$$

$$\sigma_r^{III}(r,t) = \frac{\alpha E}{1-\vartheta}\frac{1}{r^2}\left[\frac{r^2-R_{int}^2}{R_{ext}^2-R_{int}^2}G_1^{III}(r,t) - G_2^{III}(r,t)\right] \quad (65)$$

$$\sigma_r^{IV}(r,t) = \frac{\alpha E}{1-\vartheta}\frac{1}{r^2}\left[\frac{r^2-R_{int}^2}{R_{ext}^2-R_{int}^2}G_1^{IV}(t) + G_2^{IV}(r,t)\right] \quad (66)$$

$$\sigma_r^{V}(r,t) = \frac{\alpha E}{1-\vartheta}\frac{1}{r^2}\left[\frac{r^2-R_{int}^2}{R_{ext}^2-R_{int}^2}G_1^{V}(r,t) - G_2^{V}(r,t)\right] \quad (67)$$

$$\sigma_z^I(r,t) = \frac{\alpha E}{1-\vartheta}\left[\frac{2}{R_{ext}^2-R_{int}^2}G_1^I(t) - (T^I(r,t)-T_m)\right] \quad (68)$$

$$\sigma_z^{II}(r,t) = \frac{\alpha E}{1-\vartheta}\left[\frac{2}{R_{ext}^2-R_{int}^2}G_1^{II}(t) - (T^{II}(r,t)-T_m)\right] \quad (69)$$

$$\sigma_z^{III}(r,t) = \frac{\alpha E}{1-\vartheta}\left[\frac{2}{R_{ext}^2-R_{int}^2}G_1^{III}(t) - (T^{III}(r,t)-T_m)\right] \quad (70)$$

$$\sigma_z^{IV}(r,t) = \frac{\alpha E}{1-\vartheta}\left[\frac{2}{R_{ext}^2-R_{int}^2}G_1^{IV}(t) - (T^{IV}(r,t)-T_m)\right] \quad (71)$$

$$\sigma_z^{V}(r,t) = \frac{\alpha E}{1-\vartheta}\left[\frac{2}{R_{ext}^2-R_{int}^2}G_1^{V}(t) - (T^{V}(r,t)-T_m)\right] \quad (72)$$

In these equations, $G_1(t)$ and $G_2(r,t)$ terms can be explained by follows:

$$f_5(r,n) = \frac{r}{\lambda_n}\left(J_1(\lambda_n r) + H_n Y_1(\lambda_n r)\right) \quad (73)$$

$$f_6(r) = \frac{r^2}{2}(F_1(\ln(r) - 0.5) + F_2) \quad (74)$$

$$f_7(r,n) = \frac{r}{\beta_n}\left(J_1(\beta_n r) - \frac{J_1(\beta_n R_{int})}{Y_1(\beta_n R_{int})}Y_1(\beta_n r)\right) \quad (75)$$

$$G_1^I(t) = f_6(R_{ext}) - f_6(R_{int}) + \sum_{i=1}^{\infty} C_i^I e^{-\alpha\lambda_i^2 t}\left(f_5(R_{ext},i) - f_5(R_{int},i)\right) \quad (76)$$

$$G_1^{II}(t) = \sum_{i=1}^{\infty} C_i^{II} e^{-\alpha\beta_i^2 t}\left(f_7(R_{ext},i) - f_7(R_{int},i)\right) \quad (77)$$

$$G_1^{III}(t) = f_6(R_{ext}) - f_6(R_{int}) + \sum_{i=1}^{\infty} C_i^{III} e^{-\alpha\lambda_i^2 t}\left(f_5(R_{ext},i) - f_5(R_{int},i)\right) \quad (78)$$

$$G_1^{IV}(t) = \sum_{i=1}^{\infty} C_i^{IV} e^{-\alpha\beta_i^2 t}\left(f_7(R_{ext},i) - f_7(R_{int},i)\right) \quad (79)$$

$$G_1^{V}(t) = f_6(R_{ext}) - f_6(R_{int}) + \sum_{i=1}^{\infty} C_i^{V} e^{-\alpha\lambda_i^2 t}\left(f_5(R_{ext},i) - f_5(R_{int},i)\right) \quad (80)$$

$$G_1^{VI}(t) = \sum_{i=1}^{\infty} C_i^{VI} e^{-\alpha\beta_i^2 t}\left(f_7(R_{ext},i) - f_7(R_{int},i)\right) \quad (81)$$

$$G_2^I(r,t) = f_6(r) - f_6(R_{int}) + \sum_{i=1}^{\infty} C_i^I e^{-\alpha\lambda_i^2 t}\left(f_5(r,i) - f_5(R_{int},i)\right) \quad (82)$$

$$G_2^{II}(t) = \sum_{i=1}^{\infty} C_i^{II} e^{-\alpha\beta_i^2 t}\left(f_7(r,i) - f_7(R_{int},i)\right) \quad (83)$$

$$G_2^{III}(r,t) = f_6(r) - f_6(R_{int}) + \sum_{i=1}^{\infty} C_i^{III} e^{-\alpha\lambda_i^2 t}\left(f_5(r,i) - f_5(R_{int},i)\right) \quad (84)$$

$$G_2^{IV}(t) = \sum_{i=1}^{\infty} C_i^{IV} e^{-\alpha\beta_i^2 t}\left(f_7(r,i) - f_7(R_{int},i)\right) \quad (85)$$

$$G_2^{V}(r,t) = f_6(r) - f_6(R_{int}) + \sum_{i=1}^{\infty} C_i^{V} e^{-\alpha\lambda_i^2 t}\left(f_5(r,i) - f_5(R_{int},i)\right) \quad (86)$$

IV. RESULTS AND DISCUSSION

In order to provide the energy demand (Qout=5.3 kW) of the sample flat used for calculations [10], the air flow temperature is determined as Ta=347 K, 349 K and 350 K for LSC, MSC and HSC, respectively. Other parameters are n_c=14 (column number), L=2.75 m (The column height), T_m= 293 K, R_{int}=0.05m, R_{ext}=0.315 m, h_{com}=6.65 W/m^{2}K and h_{for}=171.18 W/m^{2}K (corresponding air flow of V=4 m/s) from Ref.[10]. This process is carried out for 168 hours (for a week). The charging-discharging stages are selected randomly. For seven days, the energy charging periods are selected as Δt_1=10 h, Δt_3=8h, Δt_5=7h, Δt_7=8h, Δt_9=10h, Δt_{11}=6h, Δt_{13}=9h, respectively. These values indicate energy discharging periods of Δt_2=14h, Δt_4=16h, Δt_6=17h, Δt_8=16h, Δt_{10}=14h, Δt_{12}=18 h, Δt_{14}=15h.

Figure 3 shows the Q_{out} and Q_{in} heat flux values versus the operation time. During the early moments of energy charging process, Q_{in} heat flux increases rapidly and decreases immediately. Then it decreases slowly as expected. These sudden increases and decreases at the early moments of energy charging process will show itself on the thermal stress values. The variation of Q_{out} values versus time is softener than Q_{in} curves. In addition, Figure 3 shows that the thermal energy stores heat rapidly and releases very slowly by concrete column. This thermal character of the concrete column is very important in term of its thermal energy storage potential. The effects of concrete type on Q_{out} and Q_{in} values can be ignored.

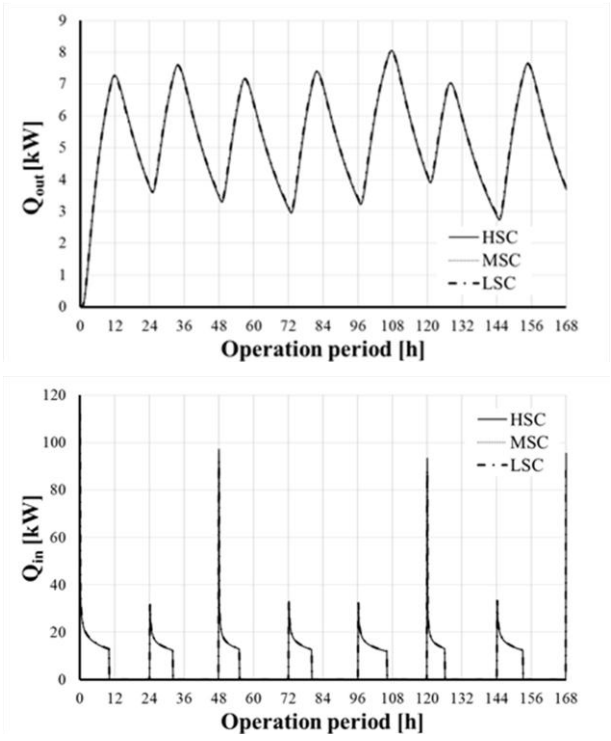

Figure 3. Variation of Qin and Qout values versus the operation period for HSC, MSC and LSC.

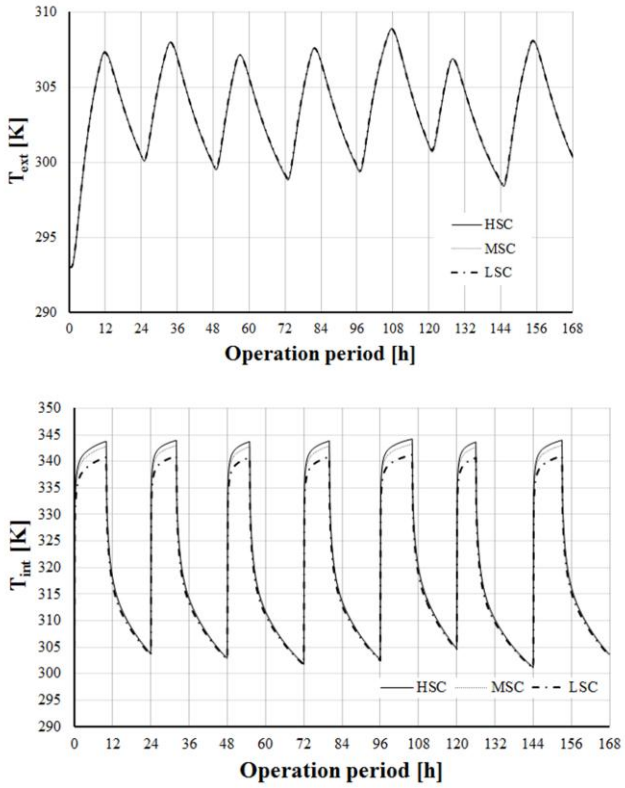

Figure 4. Variation of Tint and Text values versus the operation period for HSC, MSC and LSC

The Q_{out} results mean that indoors take thermal energy from the columns continuously the heat flux of minimum 3 kW and maximum 7 kW flows inside the room during the day corresponding to requirement of average 5.3 kW. This illustrates the energy storage ability of the concrete column and the importance of the proposed system in terms of thermal comfort.

The temperature distributions and internal surface temperatures (T_{int}) of the columns are very important for the sake safety of the suggested system. Also the temperature of columns external surfaces (T_{ext}) heating the room medium will be important in terms of thermal comfort and health. Figure 4 shows the T_{int} and Text values versus the operation time. Tint values exhibit minor changes with concrete type. The maximum temperature in the concrete occurs at the inner wall surface (r= R_{int}) of the column as $\approx$345 K for HSC and is lower than the critical safety temperature value (573 K) for concrete defined in literature [10].The hard T_{int} gradients as a function of operation time at the start and end of energy charging process from Figures 4 are important in terms of thermal stress. It well known that rapid temperature variations cause high thermal stresses. The axial thermal stress, the hoop thermal stress and the radial thermal stress profiles reached for the investigated concrete types can be seen in Figures 5, 6 and 7, respectively.

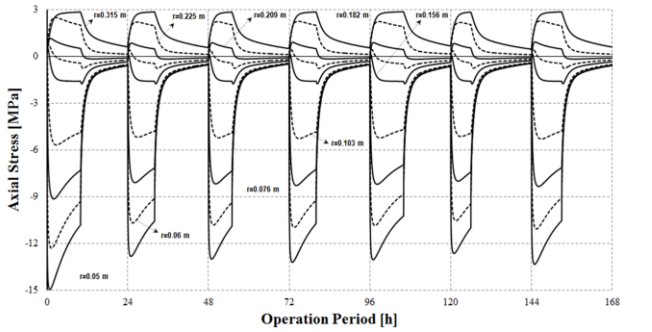

a)HSC

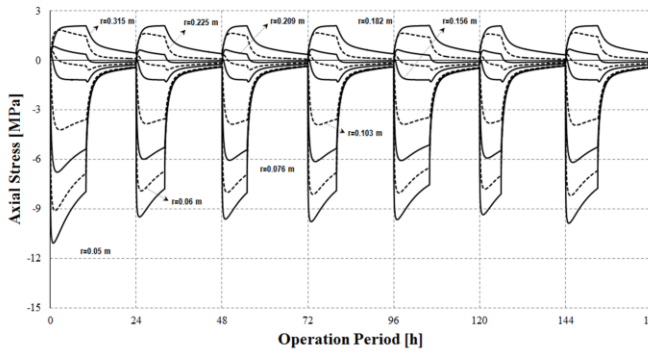

b)MSC

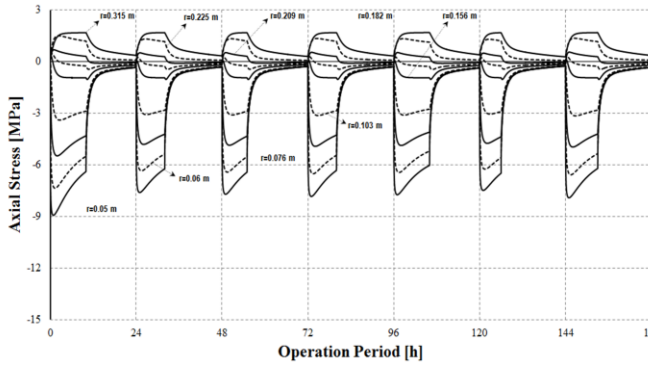

c)LSC

Figure 5. Comparison of axial stress values versus operation period

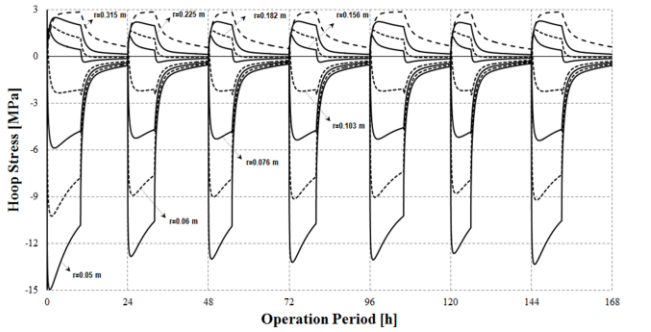

a)HSC

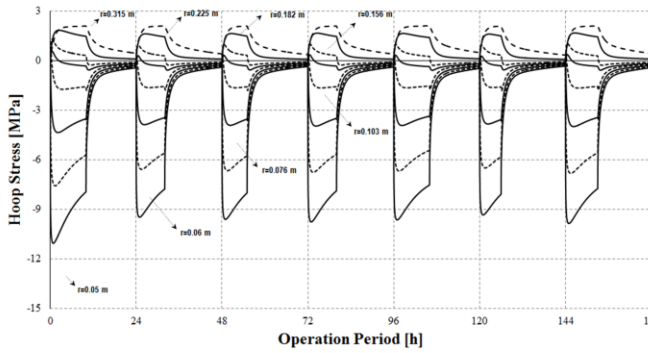

b)MSC

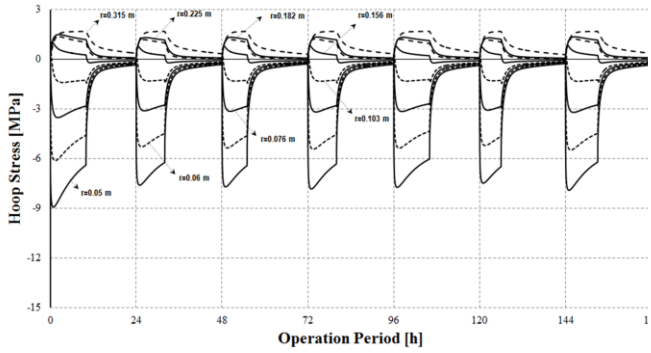

c)LSC

Figure 6. Comparison of hoop thermal stress values versus operation period

These figures show variation of the stress values at the different points (to R_{ext} from R_{int}) in the concrete column versus the operation. On the other hand, characteristic compressive strength and design compressive strength values for the concrete types can be seen in Table 5.

According to Figures 5 and 6, axial and hoop stress values are approximately the same behavior and stress values. Compressive stress at the inner regions and tensile stress at the outer regions of the column occurs. The maximum compressive and tensile stresses take place at internal and external surfaces, respectively. The maximum compressive are about 14, 10 and 7 MPa for HSC, MSC and LSC cases, respectively. On the other hand, also maximum tensile stress values are about 3, 2 and 1.5 MPa for HSC, MSC and LSC cases, respectively. These values are higher than limits of the tensile stress in Table 5. However, this risk can be easily eliminated by means of reinforcement on the external surface of the concrete column. Also according to Figure 7, radial stress values are having compressive character for all regions of the concrete column. The maximum radial stress occur about $r \approx 0.1$ m. Maximal values are about 3, 2 and 1.7 MPa for HSC, MSC and LSC cases, respectively. In the reference flat used in this and previous study [10], the concrete columns are made of concrete with compressive strength class C25. Namely, the design strength of the concrete column is calculated as 16.5 MPa [31]. This means that the hollow cylinder concrete column is already carrying nearly 17 MPa load. Therefore, the columns of the new system could not be

made from C18 (LSC) concrete class. If the columns of the new system will be made from C30 (MSC) concrete class, the difference of 3 MPa (=20-17 MPa) cannot tolerate the extra thermal load of ≈10 MPa. However, a column made from C60 (HSC) concrete class may carry the extra thermal load of ≈15 MPa because of an extra strength of 23 MPa (=40-17 MPa). Consequently, C60 concrete class will be a material that can tolerate with a double safety extra loads from thermal loading for the proposed new system. Also a concrete type (probably C50) having compressive strength of 32 MPa (=15+17 MPa) can be suggested for the new system.

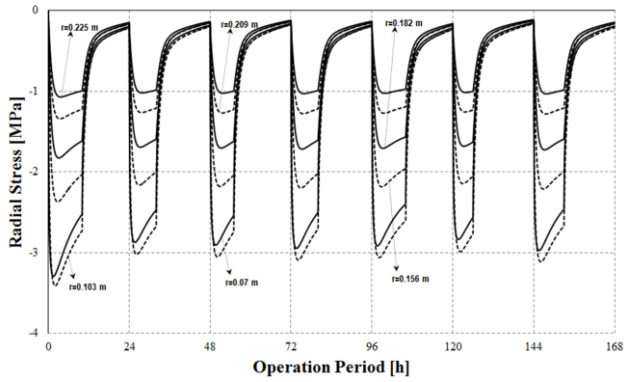

a)HSC

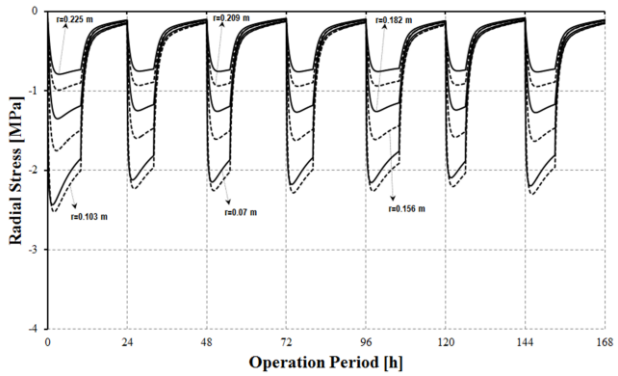

b)MSC

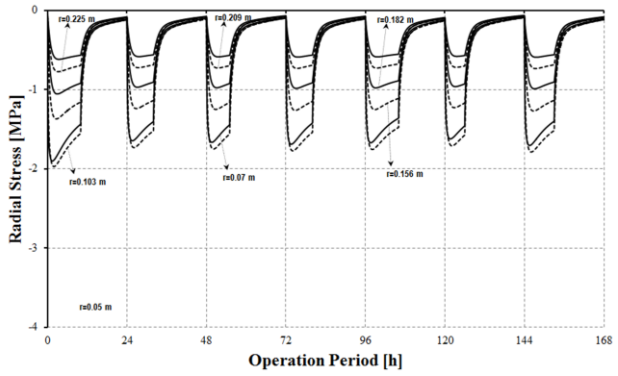

c)LSC

Figure 7. Comparison of radial thermal stress values versus operation period

TABLE IV. CHARACTERISTIC AND DESIGN COMPRESSIVE STRENGTH VALUES FOR CONCRETE TYPES

	Characteristic compressive strength fck (MPa)	*Design compressive strength fcd * (MPa)*	*Design tensile strength fctd * (MPa)*
Low strength concrete	18	12	1
Moderate strength concrete	30	20	1.28
High strength concrete	60	40	1.76

*. According to TS-500 standards [28]): fcd=fck/1.5.

V. CONCLUSIONS

In this paper, the thermal stress distribution of a concrete column, which is used as a sensible thermal energy storage medium and a heater, is investigated. An analytical solution of transient thermal stress distribution in the hollow cylinder concrete columns exposure to heat charge and discharge processes in a period of 24 hours is presented. Transient thermal calculations were carried out for three types of concrete columns made from LSC (C18), MSC (C30) and HSC (C60). The results of the calculations for sample flat showed that if a suitable concrete type is chosen in the construction stage according to the extra thermal load, the concrete columns can be used as a heater safety. For columns used as sensible thermal energy storage medium and a heater, the calculations show that the columns have to make of C50 or C60 instead of C25 which is current material. Future work should be the investigation of the effects of thermal cycling going on for years and experimental studies on concrete columns with real dimensions.

ACKNOWLEDGMENT

The authors would like to acknowledge the University of Erciyes which supported this study with project number FDK-2014-4961.

REFERENCES

[1] A Sharma, VV Tyagi, C.R. Chen, D. Buddhi, Review on thermal energy storage with phase change materials and applications, Renew. Sust. Energ. Rev., vol.13, pp.318–345,2009.

[2] N. Zhu, Z.Ma, S.Wang, Dynamic characteristics and energy performance of buildings using phase change materials: A review, Energ. Convers. Manage., vol 50, pp. 3169–3181, 2009.

[3] A. Pasupathy, R. Velraj, R.V. Seeniraj, Phase change material-based building architecture for thermal management in residential and commercial establishments, Renew. Sust. Energ. Rev., vol. 12, pp. 39–64, 2008.

[4] V.V. Tyagi, D.Buddhi, PCM thermal storage in buildings: A state of art, Renew. Sust. Energ. Rev., vol. 11, pp. 1146–1166, 2007..

[5] A.M. Khudhair, M.M. Farid, A review on energy conservation in building applications with thermal storage by latent heat using phase change materials, Energ. Convers. Manage., vol. 45, pp. 263–275, 2004.

[6] M.M. Farid, A.M. Khudhair, S.A.K. Razack, S. Al-Hallaj, A review on phase change energy storage: Materials and applications, Energ. Convers. Manage., vol. 45, pp. 1597–1615, 2004.

[7] M. Pomianowski, P. Heiselberg, Y. Zhang, Review of thermal energy storage technologies based on PCM applications in buildings, Energ. Buildings, vol. 67, pp. 58–69, 2013.

[8] A. Gracia, L.F. Cabeza, Phase change materials and thermal energy storage for Buildings, Energ. Buildings, vol. 103, pp. 414–419, 2015.

[9] J. Romanía, A. Gracia, L.F. Cabeza, Simulation and control of thermally activated building systems (TABS), Energ. Buildings, vol. 127, pp. 22–42, 2016.

[10] S. Ünalan, E. Özrahat. Concrete columns as a sensible thermal energy storage medium and a heater, Heat and Mass Transfer, vol. 50, pp. 1037-1052, 2014.

[11] V. Radu, N. Taylor, E. Paffumi, Development of new analytical solutions for elastic thermal stress components in a hollow cylinder under sinusoidal transient thermal loading, International Journal of Pressure Vessels and Piping, vol. 85, pp. 885–893, 2008.

[12] A.R. Shahani, S.M. Nabavi, Analytical solution of a quasi-static thermoelasticity problem in a pressurized thick-walled cylinder subjected to transient thermal loading, Applied Mathematical Modelling. Vol. 31, pp. 1807–18, 2007.

[13] S. Marie, Analytical expression of the thermal stresses in a vessel or pipe with cladding submitted to any thermal transient, International Journal of Pressure Vessels and Piping vol. 81, pp. 303–312, 2004.

[14] A. Kandil, A.A. EL-Kady, A. EL-Kafrawy, Transient thermal stress analysis of thick-walled cylinders, Int. J. Mech. Sci., vol. 37, pp. 721–732, 1995.

[15] J. Zhou, Z. Deng, X. Hou, Transient thermal response in thick orthotropic hollow cylinders with finite length: high order shell theory, Acta Mechanica Solida Sinica 23:156–166, 2010.

[16] P.K. Mehta, P.J.M. Monteiro, Concrete, Microstructure, Properties and Materials, Third Edition, Mc-Graw Hill, 2006.

[17] T. Mori, K. Tanaka, Average stress in matrix and average elastic energy of materials with misfitting inclusions, Acta Metallurgica, vol. 21, pp.571–574, 1973.

[18] Y. Benveniste, A new approach to the application of Mori–Tanaka's theory in composite materials, Mechanics of Materials, vol. 6, pp.147–157, 1987.

[19] V.M. Levin, Thermal expansion coefficients of heterogeneous materials, Mekh. Tverd. Tela, vol. 2, pp.88–94, 1967.

[20] J.L. Cribb, Shrinkage and thermal expansion of a two phase material, Nature, vol. 220, pp.576-577, 1968.

[21] R.A. Schapery, Thermal expansion coefficients of composite materials based on energy principles, Journal of Composite Materials, vol. 2, pp.380–404, 1968.

[22] B.W. Rosen, Z. Hashin, Effective thermal expansion coefficients and specific heats of composite materials, International Journal of Engineering Science, vol. 8, pp.157–173, 1970.

[23] H. Hatta, M. Taya, Effective thermal conductivity of a misoriented short fiber composite, Journal of Applied Physics, vol. 58, pp.2478–2486, 1985.

[24] A.M. Neville, Properties of Concrete, Fourth and Final Edition, Pearson Education Limited, 2004.

[25] E.C. Robertson, Thermal Properties of Rocks, United States Department of The Interior Geological Survey, Open-File Report , pp. 88-441, 1988.

[26] A. Abdelalim, S. Abdallah, K. Easawi, S. Negm, H. Talaat, Thermal properties of hydrated cement pastes studied by the photo acoustic technique, Journal of Physics: Conference Series vol. 21, 012136, 2010.

[27] N. Noda, R.B. Hetnarski, Y. Tanigawa, Thermal stresses, 2nd ed. Taylor & Francis, 2003.

[28] TSI (Turkish Standards Institute), TS 500-Requirements for design and construction of reinforced concrete structures. Ankara, February; 2000. (in Turkish)